Isotopic signals (^{18}O, ^{2}H, ^{3}H) of six major rivers draining the pan-Arctic watershed

Y. Yi,[1,2] J. J. Gibson,[1,2] L. W. Cooper,[3] J.-F. Hélie,[4] S. J. Birks,[5] J. W. McClelland,[6] R. M. Holmes,[7] and B. J. Peterson[8]

Received 6 July 2011; revised 9 January 2012; accepted 27 January 2012; published 22 March 2012.

[1] We present the results of a 4-year collaborative sampling effort that measured $\delta^{18}O$, $\delta^{2}H$ values and ^{3}H activities in the six largest Arctic rivers (the Ob, Yenisey, Lena, Kolyma, Yukon and Mackenzie). Using consistent sampling and data processing protocols, these isotopic measurements provide the best available $\delta^{2}H$ and ^{3}H estimates for freshwater fluxes from the pan-Arctic watershed to the Arctic Ocean and adjacent seas, which complements previous efforts with $\delta^{18}O$ and other tracers. Flow-weighted annual $\delta^{2}H$ values vary from −113.3‰ to −171.4‰ among rivers. Annual ^{3}H fluxes vary from 0.68 g to 4.12 g among basins. The integration of conventional hydrological and landscape observations with stable water isotope signals, and estimation of areal yield of ^{3}H provide useful insights for understanding water sources, mixing and evaporation losses in these river basins. For example, an inverse correlation between the slope of the $\delta^{18}O$-$\delta^{2}H$ relation and wetland extent indicates that wetlands play comparatively important roles affecting evaporation losses in the Yukon and Mackenzie basins. Tritium areal yields (ranging from 0.760 to 1.695 10^{-6} g/km^2 per year) are found to be positively correlated with permafrost coverage within the studied drainage basins. Isotope-discharge relationships demonstrate both linear and nonlinear response patterns, which highlights the complexity of hydrological processes in large Arctic river basins. These isotope observations and their relationship to discharge and landscape features indicate that basin-specific characteristics significantly influence hydrological processes in the pan-Arctic watershed.

Citation: Yi, Y., J. J. Gibson, L. W. Cooper, J.-F. Hélie, S. J. Birks, J. W. McClelland, R. M. Holmes, and B. J. Peterson (2012), Isotopic signals (^{18}O, ^{2}H, ^{3}H) of six major rivers draining the pan-Arctic watershed, *Global Biogeochem. Cycles*, *26*, GB1027, doi:10.1029/2011GB004159.

1. Introduction

[2] Dramatic changes have been observed in the Arctic hydrological cycle over the last century, including changes in the magnitude and timing of precipitation and river discharge, melting of ice on land and sea, and steric sea level changes in the Arctic Ocean [*Lewis et al.*, 2000; *Peterson et al.*, 2002; *Scharroo et al.*, 2006; *Steele and Ermold*, 2007]. These observed changes may have profound consequences with respect to global ocean circulation and climate. For example, a significant change in water column structure in the Arctic Ocean can impact the formation of North Atlantic Deep Water and consequently influence the transport and distribution of heat over the entire northern hemisphere [*Aagaard and Carmack*, 1989; *Rahmstorf*, 1995; *Peterson et al.*, 2002; *Clark et al.*, 2002]. Because there are multiple sources of freshwater inputs that sustain stratification of the Arctic Ocean, including river discharge, sea-ice meltwater, low-salinity Pacific water imported through the Bering Strait and in situ precipitation, it is important, but challenging, to distinguish and assess the transport and dynamics of individual freshwater components [*Carmack*, 2000; *Serreze et al.*, 2006; *Peterson et al.*, 2006].

[3] Water isotopes (mainly $\delta^{18}O$) have been widely used as tracers to identify and quantify freshwater components to separate water mass contribution and movement in the Arctic Ocean [e.g., *Schlosser et al.*, 2000]. The first stable isotope investigation of the Arctic Ocean was made by *Friedman et al.* [1961] as part of global surveys of water isotope compositions in natural waters. Seminal work by

[1]Alberta Innovates–Technology Futures, Victoria, British Columbia, Canada.
[2]Department of Geography, University of Victoria, Victoria, British Columbia, Canada.
[3]Chesapeake Biological Laboratory, Center for Environmental Sciences, University of Maryland, Solomons, Maryland, USA.
[4]Centre GEOTOP-UQAM, Montreal, Quebec, Canada.
[5]Alberta Innovates–Technology Futures, Calgary, Alberta, Canada.
[6]Marine Science Institute, University of Texas at Austin, Port Aransas, Texas, USA.
[7]Woods Hole Research Center, Falmouth, Massachusetts, USA.
[8]Ecosystem Center, Marine Biological Laboratory, Woods Hole, Massachusetts, USA.

0886-6236/12/2011GB004159

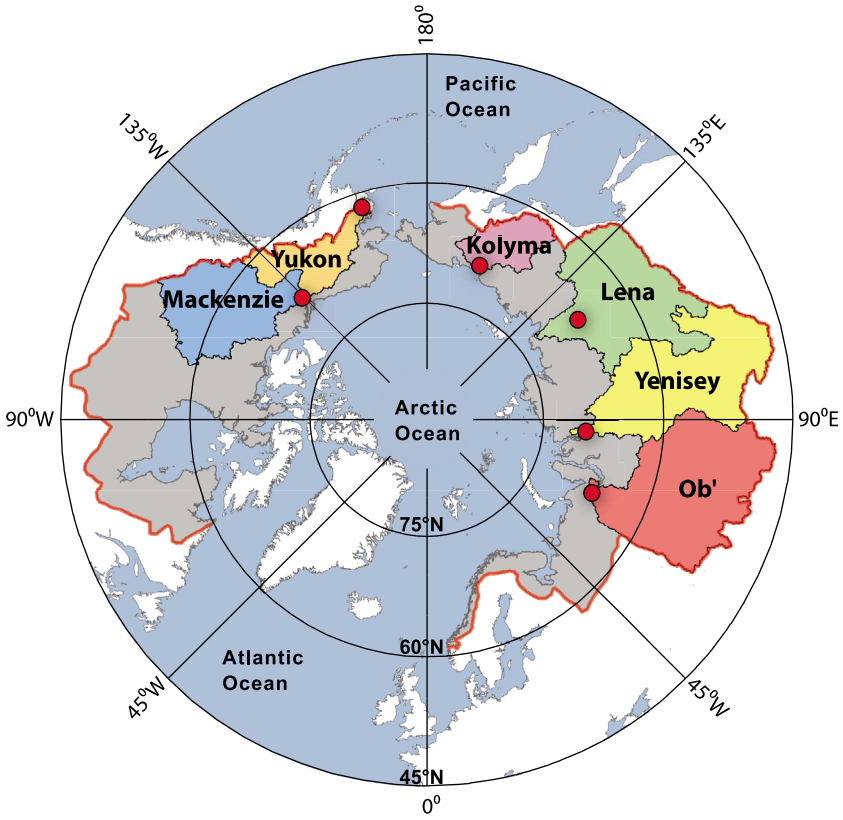

Figure 1. Circumpolar map of the six river basins sampled in this study. Outlines of the boundary of each watershed are illustrated by black solid lines. Sampling locations are indicated by red circles. The solid red line delineates the contiguous southern boundary of the area contributing freshwater into the Arctic Ocean. Although the Yukon River does not flow directly into the Arctic Ocean basin, it is an important source of freshwater input to the Arctic Ocean via transport through the Bering Strait.

Östlund and Hut [1984] subsequently demonstrated that $\delta^{18}O$ end-member analysis can be used to separate meteoric water (including runoff) from sea ice meltwater. The method was successfully used in the Canada Basin [*Macdonald et al.*, 1995; *Melling and Moore*, 1995], the Eurasian Basin [*Bauch et al.*, 1995] and across basins in the Arctic Ocean [*Ekwurzel et al.*, 2001]. Interestingly, these studies used different $\delta^{18}O$ values for the river runoff end-member. For example, *Östlund and Hut* [1984] used −21.0‰ for continental runoff based on the Global Network of Isotopes in Precipitation (GNIP). This value was subsequently used by *Melling and Moore* [1995] and *Bauch et al.* [1995]. However, *Ekwurzel et al.* [2001] estimated the overall Arctic basin river end-member composition to be −18.0‰, based upon new river data from the Ob and Yenisey while *Macdonald et al.* [1995] used values of −20.3‰ and −18.3‰ to differentiate summer and winter signatures of Mackenzie River water. This more recent differentiation reflects an appreciation that there are temporal and spatial variations in the stable isotope composition of continental runoff and that there is a need for better constraints on end-member estimates.

[4] A large data set documenting $\delta^{18}O$ values of seawater in the Arctic Ocean has become available due to collective efforts within the oceanographic research community [*Bigg and Rohling*, 2000; *LeGrande and Schmidt*, 2006]. At the same time, interdisciplinary approaches to using multiple tracers in large scale hydrological investigations are making it possible to differentiate the contributions from multiple components of continental runoff [e.g., *Guay et al.*, 2009]. Nevertheless, current estimates of isotopic end-members in these multitracer studies are often dependent upon a small number of transitory measurements, without a systematic consideration of temporal variability. When considering the inputs from high-latitude watersheds, integrating tracer signals during the spring freshet (high flow) and winter base flow (low flow) are critical for correctly labeling the fluxes of water, but these are also periods when it is challenging to obtain samples. The Pan-Arctic River Transport of Nutrients, Organic Matter and Suspended Sediments (PARTNERS) project was undertaken between 2003 and 2006 to address this shortage of seasonally explicit data for tracer concentrations in the six largest Arctic rivers by a series of coordinated sampling campaigns [*McClelland et al.*, 2008].

[5] Flow-weighted estimates of several runoff constituents ($\delta^{18}O$, DOC, Ba and alkalinity) from the PARTNERS project have been reported by *Cooper et al.* [2008]. More recently, *Holmes et al.* [2012] provide flux estimates of nutrients and organic matters (including TDN, DON, DIN, NO_3, TDP, Si and DOC) for the six rivers. Here, we report additional data on water isotope tracers, including $\delta^{18}O$, $\delta^{2}H$ and ^{3}H, which offer insights on the origin of the isotopic signals and the linkage between geomorphic features and

hydrological variations in the six largest river basins draining the pan-Arctic watershed (Figure 1).

2. Sampling and Isotopic Analysis

[6] Sampling conducted during the PARTNERS project included river water samples collected at downstream locations (but above tidal influence) that integrated the isotopic signatures of runoff from the vast majority of the drainage basin. These stations were specifically located at Salekhard (Ob River), Dudinka (Yenisey River), Zhigansk (Lena River), Cherskii (Kolyma River), Tsiigehtchic (Mackenzie River) and Pilot Station (Yukon) (Figure 1). Daily discharge for each river was measured by the United States Geological Survey (USGS, Yukon), Water Survey of Canada (Mackenzie) and Russian Federal Service of Hydrometeorology and Environmental Monitoring (Ob, Yenisey, Lena and Kolyma). Permanent gauges are not available for river stations located at Dudinka (Yenisey), Zhigansk (Lena) and Cherskii (Kolyma), so discharge from nearby gauged sites (i.e., Igarka for Yenisey, Kyusyur for Lena and Kolymskoye for Kolyma) are used for discharge records.

[7] Rivers were sampled in all seasons, in order to capture varying tracer signatures under various flow regimes, which included high-flows during the spring freshet, transient flows during summer and fall, and low-flows in winter (sampled through the ice). Between 2003 and 2006, each of the six rivers was sampled 17 times [*Holmes et al.*, 2012]. Sampling protocols followed USGS guidelines to obtain flow-weighted, depth-integrated samples at each river channel transect [*McClelland et al.*, 2008; *Cooper et al.*, 2008].

[8] During the open-water season, five sampling locations at every river transect were chosen for the deployment of depth integrating samplers (USGS D-96). The five depth-integrated samples across the river channel were then mixed in a churn to yield a single composite water sample representative of the river, and the composite sample was used for all of the laboratory analyses. For all rivers but the Yukon, the five sampling locations were chosen at equal intervals across the river channel, and the transit rate of the sampler through the water column was held constant (Equal Width Increment method according to USGS terminology). This sampling method results in a full 3-L sample at deep locations or in fast current, whereas considerable less amount of water at shallower locations or in slow currents. For the Yukon River, the channel transect was divided into five sections, each of which accounts for 20% of the total discharge (Equal Discharge Increment method according to USGS terminology). In this case, the sampler transit rate was adjusted such that a full 3-L sample was collected at each location.

[9] In contrast to the open-water season, only one location in the middle of each river channel was sampled through the ice to collect near-surface water samples for the ice-covered season. The elaborate depth-integrated sampling strategy employed during the open water season was designed particularly for accurately quantifying suspended sediment flux. This was necessary because of the uneven distribution of sediments through the water column. This is less of a concern for dissolved constituents that are more evenly mixed [*Raymond et al.*, 2007]. Thus, near-surface samples obtained during the ice-covered season are considered representative of whole river across sections, although extra caution in data interpretation may be applied.

[10] Isotopic analyses of water samples, including $\delta^{18}O$, $\delta^{2}H$ and ^{3}H concentration, were conducted at the Environmental Isotope Laboratory at the University of Waterloo. $\delta^{2}H$ in water was determined on a Continuous Flow Isotope Ratio Mass Spectrometer system, by reduction of water to H_2 gas using chromium metal as active reducing agent [*Morrison et al.*, 2001]; $\delta^{18}O$ in water was measured on a dual-inlet VG-Micromass 903 mass spectrometer via the CO_2 equilibration method [*Epstein and Mayeda*, 1953]. Results are reported in δ values (‰) relative to the international reference V-SMOW [*Coplen*, 1996]. Analytical uncertainties are $\pm$0.05‰ for $\delta^{18}O$ and $\pm$0.3‰ for $\delta^{2}H$. Water samples for ^{3}H analysis were enriched electrolytically and followed by liquid scintillation counting [*Thatcher et al.*, 1977]. Results are reported in TU (Tritium Units; 1TU = 1 tritium atom / 10^{18} hydrogen atoms, which is equivalent to 0.118 Bq/L). Typical analytical uncertainties for ^{3}H results are $\sim\pm$3%.

3. Results and Discussion

[11] Results of $\delta^{18}O$ and $\delta^{2}H$ signatures observed in the six rivers over the 4-year study are shown in Figure 2a, while flow-weighted $\delta^{18}O$ and $\delta^{2}H$ values representing input signatures from individual river basin to the sea are summarized in Table 1. Although flow-weighted $\delta^{18}O$ estimates from the PARTNERS data sets were reported previously by *Cooper et al.* [2008], $\delta^{2}H$ estimations for the six river basins are presented for the first time here. Like oxygen isotopes, hydrogen isotopes are conservative tracers of water transport. Thus, the flow-weighted $\delta^{2}H$ values reported in this paper potentially provide an additional reference for multitracer investigations in the Arctic Ocean [e.g., *Schlosser et al.*, 2000]. According to the flow-weighted estimations, the Ob, of all of the six largest rivers, contributes the most heavy-isotope enriched freshwater to the Arctic Ocean ($-$14.85 ‰ for $\delta^{18}O$ and $-$113.3 ‰ for $\delta^{2}H$), while the discharge from the Kolyma river is the least heavy-isotope enriched ($-$22.18‰ for $\delta^{18}O$ and $-$171.4 ‰ for $\delta^{2}H$). The other four rivers contribute freshwaters with intermediate isotopic signals. These isotopic distinctions between rivers are also well reflected in $\delta^{18}O$-$\delta^{2}H$ space (Figure 2a). The overall $\delta^{18}O$ and $\delta^{2}H$ pattern in Eurasian rivers is a general west-to-east decreasing trend in heavy isotope compositions, which confirms preliminary observations by *Ekwurzel* [1998].

[12] As expected, $\delta^{18}O$ values are highly correlated with $\delta^{2}H$ signatures (Figure 2a). Although seasonal fluctuations lead to overlaps in isotopic compositions, the $\delta^{18}O$-$\delta^{2}H$ correlations are strong and distinguishable among river basins (Figure 2a). In contrast to the Eurasian rivers, the two North American rivers (Yukon and Mackenzie) show conspicuous deviations from the Global Meteoric Water Line (GMWL) with significantly lower $\delta^{18}O$-$\delta^{2}H$ slopes, indicating cumulative evaporation effects. In Table 1, we provide basin-specific tabulations on $\delta^{18}O$-$\delta^{2}H$ relationships as a resource for investigators pursuing multitracer investigations.

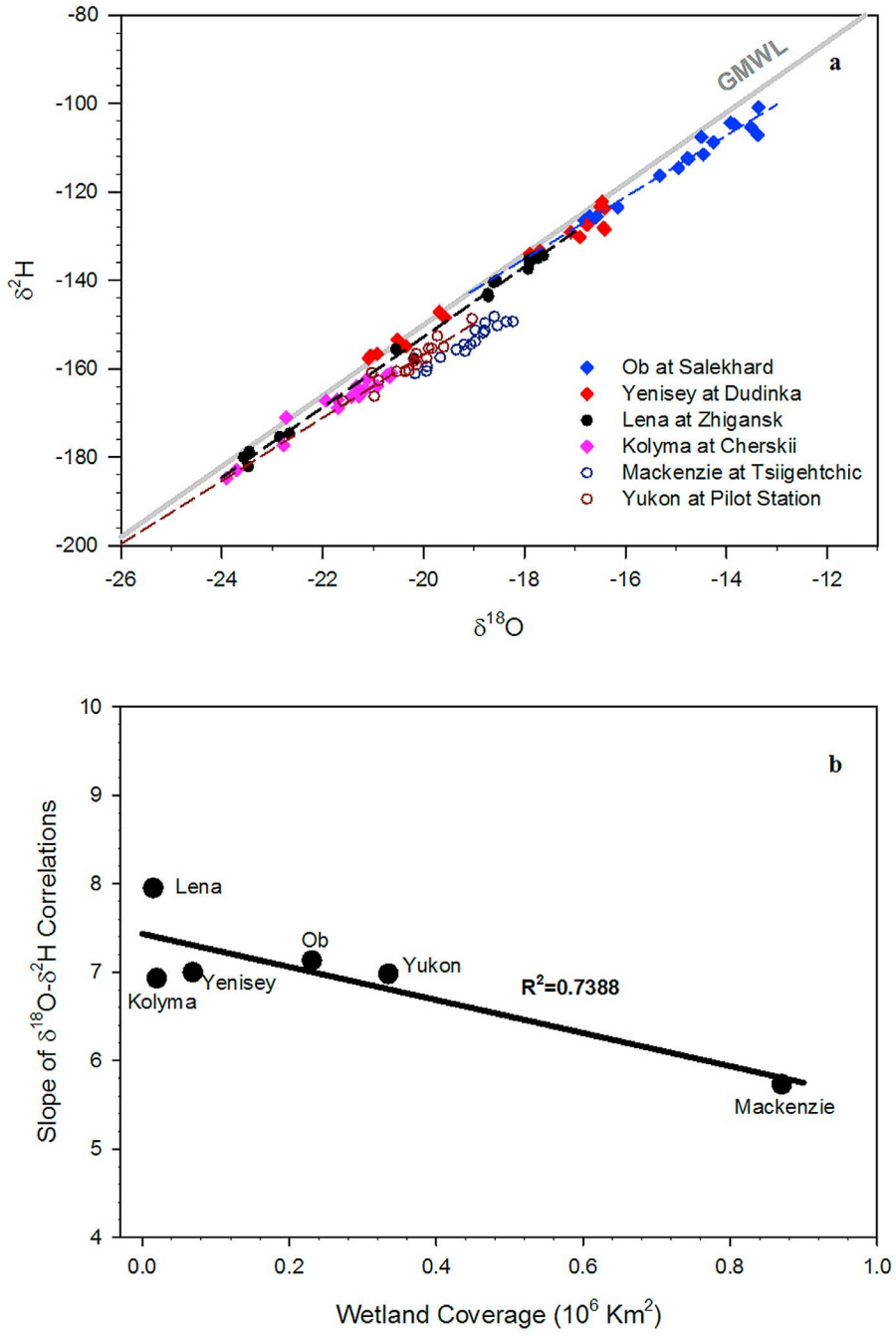

Figure 2. ^{18}O and ^{2}H signals in river discharge. (a) $\delta^{18}O$-$\delta^{2}H$ space. Results from six rivers are plotted in different colors and shapes as indicated in the legend. The solid gray line represents the Global Meteoric Water Line (GMWL). Three dashed lines are examples of basin-specific $\delta^{18}O$-$\delta^{2}H$ correlations, which are distinctive among rivers (Table 1). From the blue to black and dark brown, the three lines reflect data from the Ob, Lena and Kolyma rivers. (b) The relation between wetland coverage in river basins [*Revenga et al.*, 1998; *World Conservation Monitoring Centre*, 1998] and the slope of $\delta^{18}O$-$\delta^{2}H$ correlation (Table 1).

[13] Slopes of the $\delta^{18}O$-$\delta^{2}H$ regression lines appear to be associated with land cover features such as wetlands that are subject to evaporation (Figure 2b). River basins with the largest coverage of wetland (based upon data of *Revenga et al.* [1998] and *World Conservation Monitoring Centre* [1998]) tend to have the lowest slopes in the $\delta^{18}O$-$\delta^{2}H$ correlation. Because river discharges ultimately originate from precipitation after mixing, diffusion, and evaporation at various temporal and spatial scales, the isotopic signals in river discharge are often similar to those in precipitation, integrating large scale atmospheric processes and large scale circulation patterns [*Birks and Edwards*, 2009]. For

Table 1. A Summary of Variability and Flow-Weighted $\delta^{18}O$, $\delta^{2}H$ Values and ^{3}H Signals (Activities and Areal Yields) in the Six Rivers[a]

River	Mean Discharge (at Gauging Station) ($km^3 \cdot yr^{-1}$)	Drainage Area (at Gauging Station) (10^3 km^2)	n	$\delta^{18}O - \delta^{2}H$ Correlations	Stable Isotope Signatures				Tritium Signatures			
					Max ($\delta^{18}O$)	Min ($\delta^{18}O$)	Flux-Weighted $\delta^{18}O$	Flux-Weighted $\delta^{2}H$	Max (T.U.)	Min (T.U.)	Mean (T.U.)	Annual Mass (g)	Areal Yields (10^{-6} g/km^2)
Ob	427	2,990	17	$\delta^2H = 6.98 \times \delta^{18}O - 9.47$ ($R^2 = 0.9628$)	−13.36	−16.82	−14.85	−113.3	34.9	8.6	17.6	2.49	0.829
Yenisey	636	2,400	17	$\delta^2H = 7.04 \times \delta^{18}O - 9.32$ ($R^2 = 0.9827$)	−16.41	−21.09	−18.43	−139.4	28.1	8.7	15.6	3.27	1.363
Lena	581	2,430	17	$\delta^2H = 7.95 \times \delta^{18}O + 6.23$ ($R^2 = 0.9949$)	−17.63	−23.57	−20.47	−156.3	32.6	15.7	21.5	4.12	1.695
Kolyma	111	530	17	$\delta^2H = 6.93 \times \delta^{18}O - 17.65$ ($R^2 = 0.9503$)	−20.64	−23.91	−22.18	−171.4	23.6	12.8	18.7	0.68	1.291
Mackenzie	298	1,680	17	$\delta^2H = 5.73 \times \delta^{18}O - 44.49$ ($R^2 = 0.9249$)	−18.23	−20.53	−19.11	−153.9	18.9	11.3	13.9	1.36	0.813
Yukon	208	830	17	$\delta^2H = 7.13 \times \delta^{18}O - 14.19$ ($R^2 = 0.8949$)	−19.04	−21.60	−20.24	−158.4	12.9	3.0	9.2	0.63	0.76

[a]Drainage area is the value representing the area upstream of the discharge gauging station without scaling-up [*Holmes et al.*, 2012] to match discharge measurements at gauging station.

example, the aforementioned west-east $\delta^{18}O$ and $\delta^{2}H$ trend in Eurasian rivers likely reflects the continental effect on stable water isotopes as moisture parcels over the Eurasian continent progressively rainout from west to east. However, our results also suggest that basin-scale features can be superimposed on these-global scale signals, and can be used predictively with land surface diagnostics to understand consequences for hydrology.

[14] Variability in stable water isotope signatures of individual rivers appears to strongly correlate with variability in river discharge. Figure 3 specifically shows this for $\delta^{18}O$, while results are very similar to $\delta^{2}H$ due to the strong correlation between $\delta^{18}O$ and $\delta^{2}H$ signatures. The overall PARTNERS data set shows an inverse relationship between $\delta^{18}O$ values and specific discharge (Q). In general, as flow increases, $\delta^{18}O$ values in discharge tend to decrease (Figure 3a). However, closer examinations of individual rivers reveal that there are significant differences in response among watersheds (Figures 3b and 3c). For example, the isotopic variation in discharge in the Yenisey (Figure 3b) is apparently different from the Ob (Figure 3c). Interpretation of these different responses is, to some degree, confounded by the broad range of discharge variability among rivers. Thus, we also consider discharge anomaly (ΔQ, Figures 3d–3f) to present and explore isotopic responses to discharge variability. Mathematically, discharge anomaly is computed as $\Delta Q = \frac{Q-\chi}{\sigma}$, where Q is the instantaneous discharge; χ and σ are the mean value of discharge and the standard deviation, respectively, for the period of 2003 to 2006. ΔQ is a normalized measurement of discharge expressed relative to the mean and standard deviation, so it is essentially an index of discharge intensity [*Yi et al.*, 2010]. We observe a general trend of decreasing $\delta^{18}O$ with increasing ΔQ (Figure 3d). Moreover, two types of $\delta^{18}O$-ΔQ relation can be described for individual basins. Isotopic variation in the Yenisey, Kolyma, Mackenzie and Yukon responds to discharge intensities in a linear fashion (Figure 3e). On the other hand, isotopic variation in the Ob and Lena are decidedly nonlinear (Figure 3f). A quadratic fitting yields a significant correlation coefficient ($R^2 = 0.8757$) for the Ob River.

[15] An inverse correlation between $\delta^{18}O$ and ΔQ is expected in snowmelt-driven systems where high flows are associated with melting of the isotope-depleted snowpack, and low flows are fed by groundwater that tends to be more heavy isotope-enriched [*St. Amour et al.*, 2005; *Stadnyk et al.*, 2005; *Yi et al.*, 2010]. The strong linear correlations demonstrated in Figure 3e suggest that snowmelt is the dominant hydrological factor in four of the river basins (i.e., Yenisey, Kolyma, Yukon and Mackenzie). However, runoff generation processes for the Lena and Ob Rivers probably are more complex (Figure 3f). Instead of a gradual decrease in $\delta^{18}O$ values as flow intensity increases, the Lena $\delta^{18}O$ data demonstrate abrupt shifts between high and low flow regimes without any apparent transition. The Ob, in contrast, is well described by a quadratic response, which is similar to observations of the Liard River, a mountain-wetland transitional watershed situated within the Mackenzie Basin [*Yi et al.*, 2010]. In the Liard River, lowest flows are likely fed by groundwater, but normal flows ($\Delta Q \sim 0$) are fed by mixtures of groundwater, precipitation and surface stored water that is typically enriched in $\delta^{18}O$. Similar source

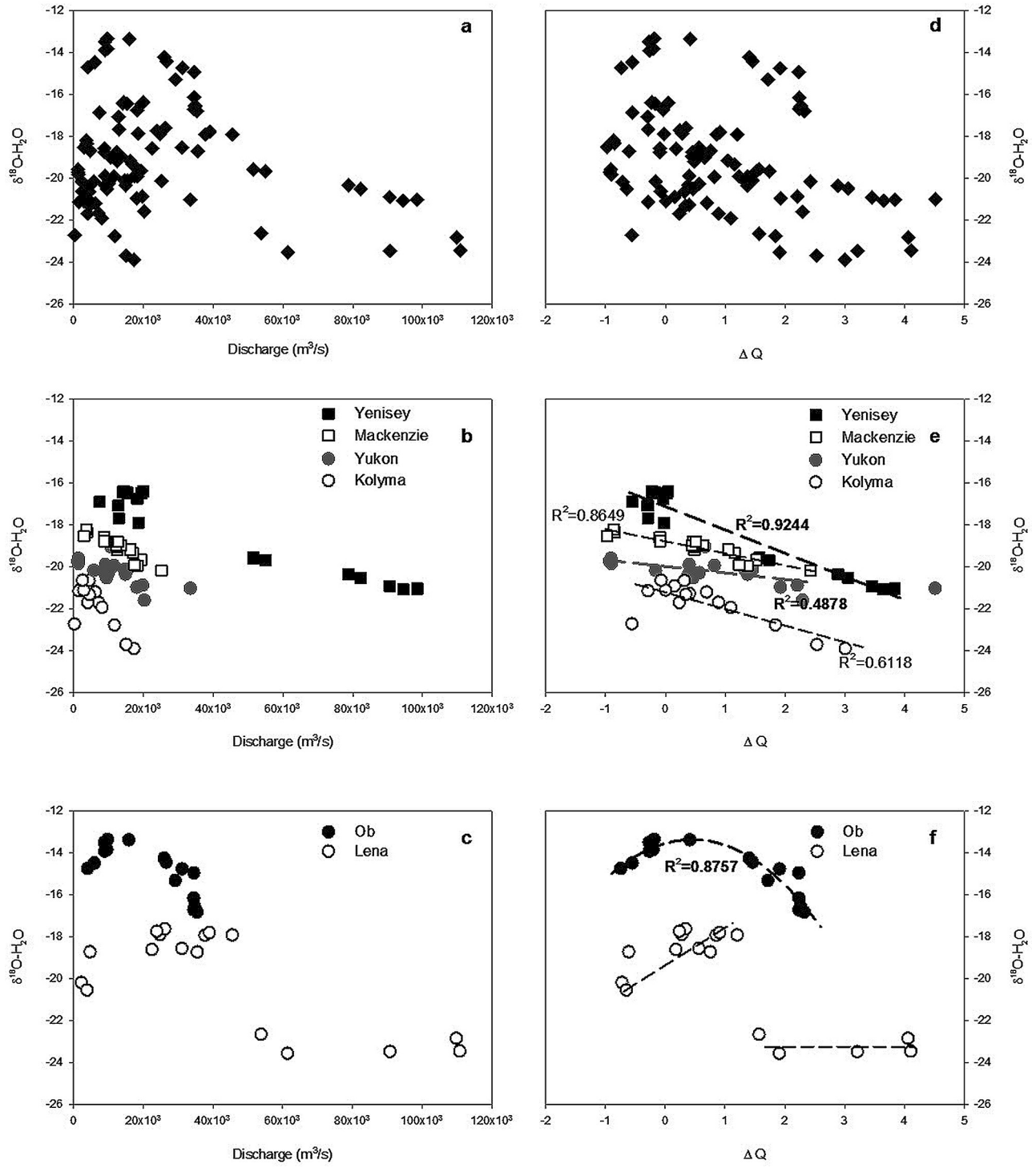

Figure 3. Isotopic response to discharge variations, showing $\delta^{18}O$ values versus discharge in six river basins. (a–c) Based on $\delta^{18}O$ versus specific discharge (Q): Figure 3a is a composite plot that does not identify individual rivers; Figures 3b and 3c are the basin-specific plots that annotate results from individual rivers as indicated by the legend. (d–e) $\delta^{18}O$ versus discharge anomaly (ΔQ): Figure 3d is a composite plot that does not identify individual rivers; Figures 3e and 3f are the basin-specific plots that annotate results from individual rivers.

mixtures may explain the initial increase in $\delta^{18}O$ values in both the Ob and Lena basins as ΔQ increases from -1 to 0. The quadratic overturn in the $\delta^{18}O$-ΔQ relationship for the Ob is likely driven by proportional increases in the snowmelt contribution, as would be the case in a snowmelt influenced system. At extremely high flow conditions ($\Delta Q \geq 2$), the Lena basin discharge had consistent, very low $\delta^{18}O$ values ($\sim -23.20‰$), which is a different response from all other

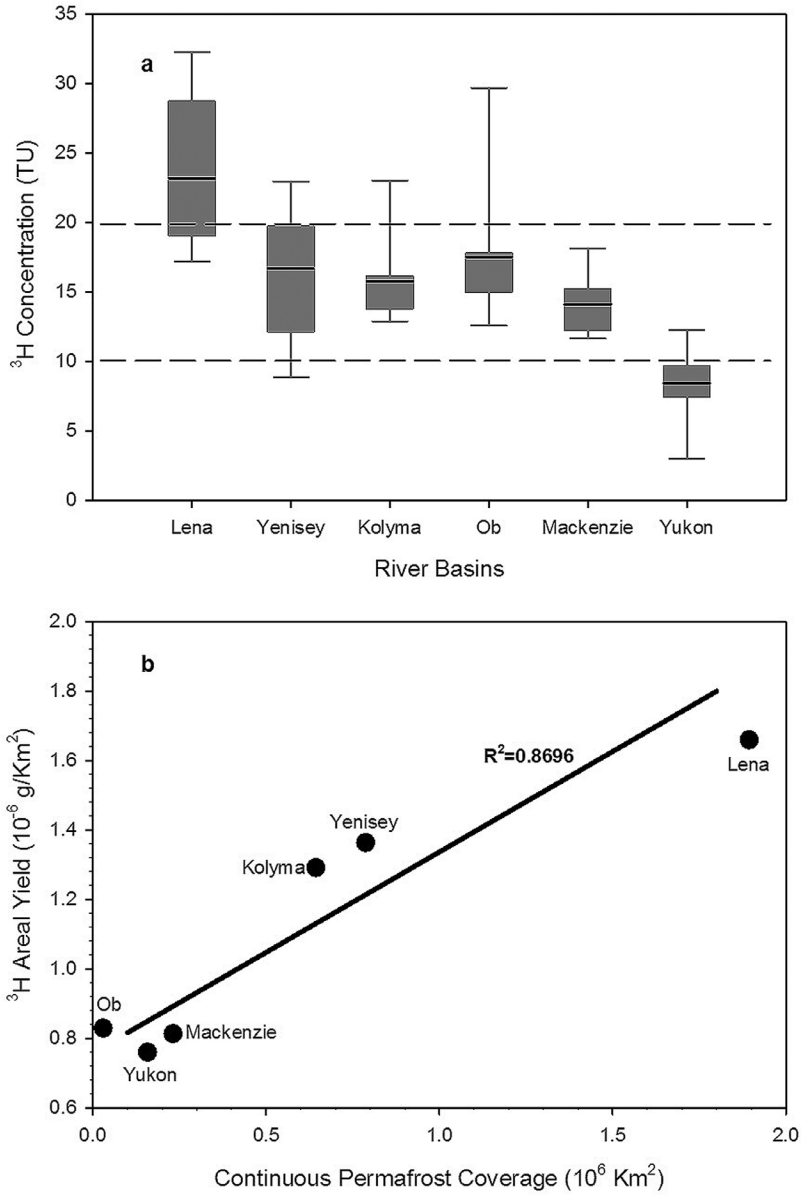

Figure 4. ^{3}H signals in river discharge. (a) The box-whisker plot of tritium concentration measured in each river. (b) The correlation between continuous permafrost coverage [*Holmes et al.*, 2012] and the estimated areal yields (Table 1) for individual river basins.

rivers. These data suggest that dominance of snowmelt runoff may be seasonally longer in the Lena basin and the transition to summer precipitation and groundwater contributions is not as gradual as those in other basins. Apparently, hydrological variations are not driven by snowmelt only in northern rivers, although it is important in all six rivers.

[16] In addition to δ^{18}O and δ^2H results, ^{3}H concentrations are also reported here. The highest ^{3}H concentration (34.9 TU) was measured in the Ob River, while the lowest ^{3}H concentration (3.0 TU) was observed in the Yukon River (Table 1). The statistical distributions among river basins are presented in Figure 4a. *Fourré et al.* [2006] estimated recent natural background concentrations of tritium in precipitation in the high-latitude northern hemisphere to be between 10 and 20 TU. Although there are occasional observations of high or low ^{3}H activities beyond expected background ranges in four of the six rivers (Yenisey, Ob, Mackenzie and Kolyma), such as 34.9 TU in the Ob basin during the summer of 2005, these four rivers are generally within expected background range after considering statistical means. The Lena had anomalously high mean ^{3}H concentrations, while the Yukon had anomalously low mean ^{3}H concentrations (Figure 4a).

[17] The mass flux of tritium through each river basin was estimated using tritium concentrations and specific discharges. Flow weighting of the mean concentration of ^{3}H in the rivers results in an estimated total contribution of ~12.55 g/year of tritium from the six rivers to the Arctic Ocean (Table 1). Estimates for the ^{3}H mass contributions

from individual basins (ranging from 0.63 g to 4.12 g) are comparable to those from the Mississippi River, which is on the order of 1–2 g per year [*Michel*, 2004]. The tritium fluxes from individual basins are most usefully compared by scaling the mass flux to the size of the river basin (mass flux per contributing area, also referred as areal yield in Table 1). The Lena, Yenisey and Kolyma drainage basins have high tritium areal yields, 1.695×10^{-6}, 1.363×10^{-6} and 1.291×10^{-6} g/km^2 respectively, whereas the other three drainage basins have relatively low ($\sim 0.8 \times 10^{-6}$ g/km^2) tritium areal yields. High concentrations and high areal yields in the mid-continental Eurasian basins (Lena, Yenisey and Kolyma; Table 1) are consistent with previous observations that mid-continental locations (despite draining northward into the Arctic) have higher concentrations of tritium in precipitation and subsequently in river discharges [*Vakulovskii et al.*, 1978; *Michel*, 2004]. In contrast, the tritium concentrations measured in the Yukon River are lower than those in modern precipitation and consistent with other longer-term tritium measurements (R. Michel, USGS, personal communication, 2009). Areal yield estimates from Yukon River basin are also the lowest among the six studied river basins. It is reasonable to expect that this is due to dilution by tritium-free glacial meltwater in the Yukon basin, which is a much less important component in the other studied river basins. Also of interest, we found that areal yields of tritium appear to be strongly correlated with differences in coverage of continuous permafrost among basins (Figure 4b). High areal yield basins (>1.0×10^{-6} g/km^2) are those with vast coverage of permafrost (>0.6M km^2). The increase in areal yield seems to be proportional to the increase in basin-wide permafrost. On the other hand, in basins where areal yield of tritium clustered around 0.8×10^{-6} g/km^2 (Ob, Yukon and Mackenzie), permafrost is proportionally a less important landscape feature. In general, permafrost inhibits infiltration and reduces response times in runoff generation [*Woo*, 1986], which may contribute to high tritium yields. However, understanding the underlain mechanism linking permafrost with ^{3}H areal yield will require further study. In any case, tritium seems to be a sensitive tracer to changes in permafrost, especially when near-surface permafrost in the circumpolar Arctic is anticipated to degrade significantly [*Frey and McClelland*, 2009].

[18] There are isotopic observations linking landscape characteristics with hydrological responses. For instance, the importance of wetlands in contributing to cumulative evaporation is supported by the strong correlation between wetland coverage and δ^{18}O-δ^2H correlation slopes (Figure 2b); the potential impacts of permafrost degradation are reflected by correlations between permafrost coverage and ^{3}H areal yields (Figure 4b). It is also important to note that diverse landcover features contribute to integrated signals in northern rivers and different tracers label and track processes with distinct emphases. Therefore, a drainage-specific approach with targets on landscape features may be strategic for designing a monitoring program in the circumpolar Arctic. Our observations suggest that permafrost dominated basins such as Lena with high ^{3}H areal yields could be investigated productively via ^{3}H monitoring and relating ^{3}H signatures to permafrost processes. In contrast, monitoring hydrological change in the Yukon and Mackenzie basins could profit from attention to the role of wetlands and numerous large lakes where δ^{18}O and δ^2H values, appear to record watershed-wide water balance budgets.

4. Concluding Remarks

[19] Flow-weighted isotopic signatures (δ^{18}O, δ^2H and ^{3}H), as well as river specific δ^{18}O-δ^2H correlations, provide a useful context for understanding the continental discharge of individual rivers to the Arctic Ocean. For the first time, we report flow-weighted δ^2H values, basin-specific δ^{18}O-δ^2H correlations, and ^{3}H areal yields for individual river basins. Better constraints on water tracers in the six largest Arctic rivers improve the capacity to separate freshwater contributions to the Arctic Ocean, especially the possibility for better region-based analyses in the Eurasian and North American basins. Two types of isotopic variability in response to hydrological variations for the six pan-Arctic rivers (one was linear, and the other was nonlinear in relation to discharge intensity ΔQ), highlight the variability and complexity of hydrological processes in Arctic drainage basins. Our results indicate that high latitude hydrological processes are not always driven by a single factor (e.g., snowmelt). Furthermore, apparent correlations among isotopic signals, permafrost coverage, and wetland extent suggest potential linkages between landscape characteristics and hydrological responses. With growing evidence of possible changes in the relative importance of surface versus groundwater in the pan-Arctic region, the role of permafrost (an effective recharge barrier) and the role of wetlands (an effective buffer of water movement) should be accorded more attention in scaled studies. Coordinated efforts using the PARTNERS model should be continued to compare and document basin-specific changes.

[20] **Acknowledgments.** We thank the PARTNERS field team for field efforts that made this valuable data set available. We are also grateful to the Environmental Isotope Laboratory - at the University of Waterloo for undertaking the stable water isotope and tritium analysis of water samples. Funding for this research was provided by the U.S. National Science Foundation (OPP-0229302), the National Science and Engineering Research Council of Canada (Discovery grant to JJG and IRD fellowship to YY), the U.S. Geological Survey and the Water Resources Division in the Department of Indian Affairs and Northern Development, Canada. We especially thank S. Jasechko, two anonymous reviewers and the editor for their helpful comments that improved an earlier version of the manuscript.

References

Aagaard, K., and E. C. Carmack (1989), The role of sea ice and other fresh water in the arctic circulation, *J. Geophys. Res.*, *94*, 14,485–14,498, doi:10.1029/JC094iC10p14485.

Bauch, D., P. Schlosser, and R. G. Fairbanks (1995), Freshwater balance and the sources of deep and bottom waters in the Arctic Ocean inferred from the distribution of $H_2^{18}O$, *Prog. Oceanogr.*, *35*, 53–80, doi:10.1016/0079-6611(95)00005-2.

Bigg, G. R., and E. J. Rohling (2000), An oxygen isotope data set for marine waters, *J. Geophys. Res.*, *105*, 8527–8535, doi:10.1029/2000JC900005.

Birks, S. J., and T. W. D. Edwards (2009), Atmospheric circulation controls on precipitation isotope-climate relations in western Canada, *Tellus, Ser. B*, *61*, 566–576, doi:10.1111/j.1600-0889.2009.00423.x.

Carmack, E. C. (2000), The Arctic Ocean's freshwater budget: Sources, storage and export, in *The Freshwater Budget of the Arctic Ocean*, edited by E. L. Lewis, pp. 91–126, Kluwer Acad., Dordrecht, Netherlands.

Clark, P. U., U. G. Pisias, T. F. Stocker, and A. J. Weaver (2002), The role of the thermohaline circulation in abrupt climate change, *Nature*, *415*, 863–869, doi:10.1038/415863a.

Cooper, L. W., J. W. McClelland, R. M. Holmes, P. A. Raymond, J. J. Gibson, C. K. Guay, and B. J. Peterson (2008), Flow-weighted values of runoff

tracers ($\delta^{18}O$, DOC, Ba, alkalinity) from the six largest Arctic rivers, *Geophys. Res. Lett.*, *35*, L18606, doi:10.1029/2008GL035007.

Coplen, T. B. (1996), New guidelines for reporting stable hydrogen, carbon, and oxygen isotope-ratio data, *Geochim. Cosmochim. Acta*, *60*, 3359–3360, doi:10.1016/0016-7037(96)00263-3.

Ekwurzel, B. (1998), Arctic Ocean water mass circulation and ventilation ages derived from tritium, helium and oxygen-18 tracers, PhD thesis, Columbia Univ., New York.

Ekwurzel, B., P. Schlosser, R. A. Mortlock, R. G. Fairbanks, and J. H. Swift (2001), River runoff, sea ice meltwater, and Pacific water distribution and mean residence times in the Arctic Ocean, *J. Geophys. Res.*, *106*, 9075–9092, doi:10.1029/1999JC000024.

Epstein, S., and T. Mayeda (1953), Variation of ^{18}O content of water from natural sources, *Geochim. Cosmochim. Acta*, *4*, 213–224, doi:10.1016/0016-7037(53)90051-9.

Fourré, E., P. Jean-Baptiste, A. Dapoigny, D. Baumier, J. R. Petit, and J. Jouzel (2006), Past and recent tritium levels in Arctic and Antarctic polar caps, *Earth Planet. Sci. Lett.*, *245*, 56–64, doi:10.1016/j.epsl.2006.03.003.

Frey, K. E., and J. W. McClelland (2009), Impacts of permafrost degradation on arctic river biogeochemistry, *Hydrol. Processes*, *23*, 169–182, doi:10.1002/hyp.7196.

Friedman, I., B. Schoen, and J. Harris (1961), The deuterium concentration in Arctic sea ice, *J. Geophys. Res.*, *66*, 1861–1864, doi:10.1029/JZ066i006p01861.

Guay, C. K. H., F. A. McLaughlin, and M. Yamamoto-Kawai (2009), Differentiating fluvial components of upper Canada Basin waters on the basis of measurements of dissolved barium combined with other physical and chemical tracers, *J. Geophys. Res.*, *114*, C00A09, doi:10.1029/2008JC005099.

Holmes, R. M., et al. (2012), Seasonal and annual fluxes of nutrients and organic matter from large rivers to the Arctic Ocean and surrounding seas, *Estuaries Coasts*, doi:10.1007/s12237-011-9386-6, in press.

LeGrande, A. N., and G. A. Schmidt (2006), Global gridded data set of the oxygen isotopic composition in seawater, *Geophys. Res. Lett.*, *33*, L12604, doi:10.1029/2006GL026011.

Lewis, E. L., E. P. Jones, P. Lemke, T. D. Prowse, and P. Wadhams (2000), *The Freshwater Budget of the Arctic Ocean*, 623 pp., Kluwer Acad., Dordrecht, Netherlands.

Macdonald, R. W., D. W. Paton, E. C. Carmack, and A. Omstedt (1995), The freshwater budget and under-ice spreading of Mackenzie River water in the Canadian Beaufort Sea based on salinity and $^{18}O/^{16}O$ measurements in water and ice, *J. Geophys. Res.*, *100*, 895–919, doi:10.1029/94JC02700.

McClelland, J. W., et al. (2008), Development of Pan-Arctic database for river chemistry, *Eos Trans. AGU*, *89*, 217–218, doi:10.1029/2008EO240001.

Melling, H., and R. M. Moore (1995), Modification of halocline source waters during freezing on the Beaufort Sea Shelf: Evidence from oxygen isotopes and dissolved nutrients, *Cont. Shelf Res.*, *15*, 89–113, doi:10.1016/0278-4343(94)P1814-R.

Michel, R. L. (2004), Tritium hydrology of the Mississippi River basin, *Hydrol. Processes*, *18*, 1255–1269, doi:10.1002/hyp.1403.

Morrison, J., T. Brockwell, T. Merren, F. Fourel, and A. M. Philips (2001), On-line high precision stable hydrogen isotopic analyses on nanoliter water samples, *Anal. Chem.*, *73*, 3570–3575, doi:10.1021/ac001447t.

Östlund, H. G., and G. Hut (1984), Arctic Ocean water mass balance from isotope data, *J. Geophys. Res.*, *89*, 6373–6381, doi:10.1029/JC089iC04p06373.

Peterson, B. J., R. M. Holmes, J. W. McClelland, C. J. Vorosmarty, R. B. Lammers, A. I. Shiklomanov, and S. Rahmstorf (2002), Increasing river discharge to the Arctic Ocean, *Science*, *298*, 2171–2173, doi:10.1126/science.1077445.

Peterson, B. J., J. W. McClelland, R. Curry, R. M. Holmes, J. Walsh, and K. Aagaard (2006), A trajectory shift in the arctic and subarctic freshwater cycle, *Science*, *313*, 1061–1066, doi:10.1126/science.1122593.

Rahmstorf, S. (1995), Bifurcations of the Atlantic thermohaline circulation in response to changes in the hydrological cycle, *Nature*, *378*, 145–149, doi:10.1038/378145a0.

Raymond, P. A., J. M. McClelland, R. M. Holmes, A. V. Zhulidov, K. Mull, B. J. Peterson, R. G. Striegl, G. R. Aiken, and T. Y. Gurtovaya (2007), Flux and age of dissolved organic carbon exported to the Arctic Ocean: A carbon isotopic study of the five largest arctic rivers, *Global Biogeochem. Cycles*, *21*, GB4011, doi:10.1029/2007GB002934.

Revenga, C., S. Murray, J. Abramovitz, and A. Hammond (1998), *Watersheds of the World: Ecological Value and Vulnerability*, World Resour. Inst., Washington, D. C.

Scharroo, R., A. L. Ridout, and S. W. Laxon (2006), Arctic sea level change from satellite altimetry, *Eos Trans. AGU*, *87*(36), Jt. Assem. Suppl., Abstract G21A-02.

Schlosser, P., B. Ekwurzel, S. Khatiwala, B. Newton, W. Maslowski, and S. Pfirman (2000), Tracer studies of the arctic freshwater budget, in *The Freshwater Budget of the Arctic Ocean*, edited by E. L. Lewis, pp. 453–478, Kluwer Acad., Dordrecht, Netherlands.

Serreze, M. C., P. B. Andrew, A. G. Slater, R. A. Woodgate, K. Aagaard, R. B. Lammers, M. Steele, R. Moritz, M. Meredith, and C. M. Lee (2006), The large-scale freshwater cycle of the Arctic, *J. Geophys. Res.*, *111*, C11010, doi:10.1029/2005JC003424.

Stadnyk, T. A., N. A. St. Amour, N.Kouwen, T. W. D. Edwards, T. D. Prowse, A. Pietroniro, and J. J. Gibson (2005), A groundwater separation study in boreal wetland terrain: The WATERFLOOD hydrological model compared with stable isotope tracers, *Isotopes Environ. Health Stud.*, *41*, 49–68, doi:10.1080/10256010500053730.

St. Amour, N. A., J. J. Gibson, T. W. D. Edwards, T. D. Prowse, and A. Pietroniro (2005), Isotopic time-series partitioning of streamflow components in wetland-dominated catchments, lower Liard River Basin, Northwest Territories, Canada, *Hydrol. Processes*, *19*, 3357–3381, doi:10.1002/hyp.5975.

Steele, M., and W. Ermold (2007), Steric sea level change in the Northern Seas, *J. Clim.*, *20*(3), 403–417, doi:10.1175/JCLI4022.1.

Thatcher, L. L., V. J. Janzer, and K. W. Edwards (1977), Methods for determination of radioactive substances in water and fluvial sediments, *U.S. Geol. Surv. Tech. Water Resour. Invest.*, *Book 5*, *Chap. A5*, 79–81.

Vakulovskii, S., A. I. Vorontsov, I. Y. Katrich, I. A. Koloskov, F. Y. Rovinskii, and E. I. Roslyi (1978), Tritium in atmospheric precipitations, rivers and seas in and around the USSR Territory, *At. Energiya*, *44*, 432–435.

Woo, M. K. (1986), Permafrost hydrology in North America, *Atmos. Ocean*, *24*, 201–234, doi:10.1080/07055900.1986.9649248.

World Conservation Monitoring Centre (1998), *Biodiversity Map Library*, U. N. Environ. Programme, Cambridge, U. K.

Yi, Y., J. J. Gibson, J.-F. Hélie, and T. A. Dick (2010), Synoptic and time-series stable isotope surveys of the Mackenzie River from Great Slave Lake to the Arctic Ocean, 2003 to 2006, *J. Hydrol.*, *383*, 223–232, doi:10.1016/j.jhydrol.2009.12.038.

S. J. Birks, Alberta Innovates–Technology Futures, Calgary, AB T2L 2A6, Canada.

L. W. Cooper, Chesapeake Biological Laboratory, Center for Environmental Sciences, University of Maryland, Solomons, MD 20688, USA.

J. J. Gibson and Y. Yi, Alberta Innovates–Technology Futures, Vancouver Island Technology Park, Victoria, BC V8Z 7X8, Canada.

J.-F. Hélie, Centre GEOTOP-UQAM, Montreal, QC H2X 3Y7, Canada.

R. M. Holmes, Woods Hole Research Center, Falmouth, MA 02540, USA.

J. W. McClelland, Marine Science Institute, University of Texas at Austin, Port Aransas, TX 78373, USA.

B. J. Peterson, Ecosystem Center, Marine Biological Laboratory, Woods Hole, MA 02543, USA.